UDC 622.831: 624.131 DOI: https://doi.org/10.15407/geotm2025.175.025

MATHEMATICAL MODEL FOR CALCULATING THE PARAMETERS OF DIAGRAMS OF CRUSHING CYLINDRICAL SAMPLES OF ROCK SPECIES WITH THEIR WEDGE-SHAPED FORM OF DESTRUCTION

Vasyliev D., Tynyna S., Kress D., Rizo Z., Kulak Ye.

M.S. Poliakov Institute of Geotechnical Mechanics of the National Academy of Sciences of Ukraine

Abstract. Managing the stress-strain state of rock masses will enable the prediction and assurance of safe mining operations during the exploitation of enterprises. Therefore, the authors of the article have established that one of the key characteristics that are significant for controlling the stress-strain state of rock masses and ensuring their effective destruction during disintegration are the strength limit and residual strength indicators of the samples. These parameters are determined based on diagrams that reflect the dependence of normal stress on longitudinal deformation during the ultimate destruction of materials. It should also be noted that the results of the studies conducted are needed directly at the mining enterprise to make decisions based on the information obtained about the properties of rocks, and this equipment is not available at the sites themselves. The purpose of the article is to develop an analytical method for calculating the parameters of cylindrical rock sample crushing diagrams based on their wedge-shaped failure mode in order to control the stress-strain state of the rock mass and increase the efficiency of failure during disintegration. The authors analytically modelled the process of destruction of cylindrical rock samples during wedge-shaped destruction using experimental values of four rock property indicators: shear strength, internal and external friction coefficients, and elastic modulus. The limits and residual strength of the samples are equivalent to analytical data calculated from the normal stress-longitudinal strain diagrams obtained on pressing equipment. Comparison of the calculated strength limits with the experimental results confirmed the reliability of the developed method with an accuracy of 82–85%.

For the first time, analytical modelling of the destruction process of cylindrical rock samples caused by wedge-shaped destruction has been performed, taking into account internal and external friction factors. The proposed method allows determining the parameters of stress-strain diagrams of cylindrical rock samples with wedge-shaped destruction using four property indicators that can be easily established experimentally in mining conditions, where the calculation results can be quickly used to assess the effectiveness of destruction during disintegration.

Keywords: rock, strength limit, destruction, crack, "stress-strain" diagram

1. Introduction

The effective operation of mining enterprises engaged in both open-pit and underground mineral extraction determines the sustainable development of industrial regions such as the Lviv-Volyn Basin, Western Donbas, Kryvbas, and others.

Mining at great depths leads to changes in the stress-strain state of the rock mass, an increase in rock pressure, which entails deformation of the earth's surface, shifts, subsidence, the formation of voids, and the development of fracturing in the rock mass.

Controlling the stress-strain state of the rock mass will make it possible to predict and ensure the safe development of mining operations during the exploitation of enterprises.

One of the key characteristics that are important for managing the stress-strain state of rock mass and ensuring its effective destruction during disintegration are the strength limit and residual strength indicators of samples [1–5]. These parameters are determined based on diagrams that reflect the dependence of normal stress on longitudinal deformation during the ultimate failure of materials [6–8].

To control the stress-strain state of rock masses and ensure their effective disintegration, it is necessary to know the strength limit and residual strength of samples, determined from the “longitudinal stress-strain” diagrams of their ultimate failure.

Received: 08.05.2025 Accepted: 15.12.2025 Available online: 19.12.2025

Prismatic or cylindrical samples are used for the experimental determination of rock failure diagram parameters [8–10]. Methods for the analytical determination of parameters for prismatic samples are described in detail in [11]. However, in practice, cylindrical samples obtained from core drilling are used more often than prismatic ones. This creates a need for analytical methods for calculating the strength of cylindrical samples.

2. Methods

Under uniaxial compression of cylindrical samples, a wedge-shaped fracture pattern is observed (Fig. 1).

The analytical determination of the strength of samples with this type of failure can be performed using the proposed methodology. To characterize the process of rock failure, Coulomb's criterion is effectively applied, which is based on the maximum effective tangential stresses arising on slip lines or, more preferably, on slip surfaces (SS). In works [12–18], Coulomb's criterion for cohesive media is based on the assumption that the shear resistance of rock τα on the inclined surface under consideration is determined as the sum of two factors: the ultimate strength in pure shear and a component proportional to the normal stress σ_α on this surface (with compression considered positive), which is caused by internal friction.

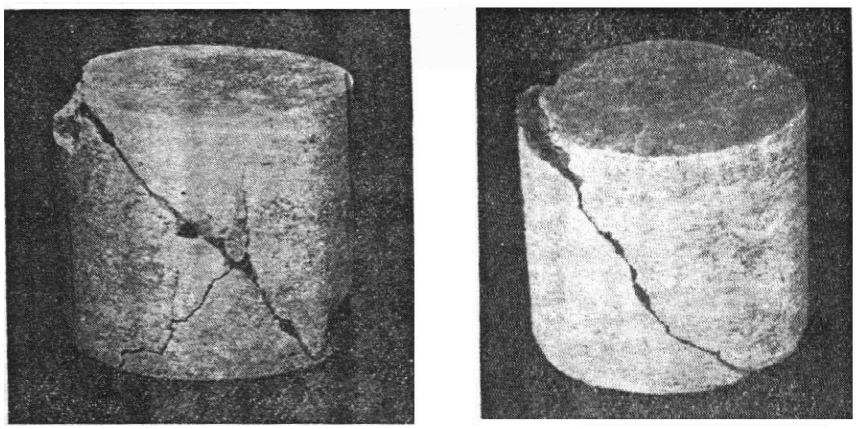

pyramidal form diagonal form

Figure 1 – Forms of rock sample destruction according to Baron L.I.

When the sample is destroyed on the SS, a crack forms. As it develops, part of the material loses its connection with the load area. Based on the flat deformation model, the remaining load-bearing part of the sample material can be determined at any given moment by the known position of the tip of one or two cracks. This value corresponds to the initial area of the sample minus the area freed from load as a result of crack growth along the SS. The part of the sample freed from load will correspond to the values of the abscissa of the crack tip as $x = yctg\alpha$, where y – ordinate of the OY axis, α – angle of inclination of SS at the crack tip relative to the x-axis. Taking into account the stresses σ_y at the crack tip, its coordinates, and the patterns of the contact stress distribution function on the main part of the sample, it is possible to develop a

method for calculating the parameters of fracture diagrams based on Coulomb's criterion. This approach requires data on four key characteristics of the material: shear strength, external (contact) and internal friction coefficients, and elastic modulus.

First, let us consider the concept of test specimen failure. Figure 2 shows a diagram of a specimen subjected to a vertical load, Figure 2 shows a diagram of a sample subjected to vertical loading, where m is the point of failure. In addition, the specimen is subject to τ_c – contact tangential stresses arising from friction and directed inward, counteracting transverse deformation, m – fracture initiation point. The coordinate system is defined with its center at the upper left corner of the specimen. On the upper surface of the left longitudinal part of the specimen, the tangential stresses are positive, while on the lower side, negative values are recorded. For the right half, the signs are reversed. It is important to note that under the action of a vertical load, the specimen takes on a convex shape. Due to this, the rule of parity of tangential stresses becomes applicable at the corners of the specimen.

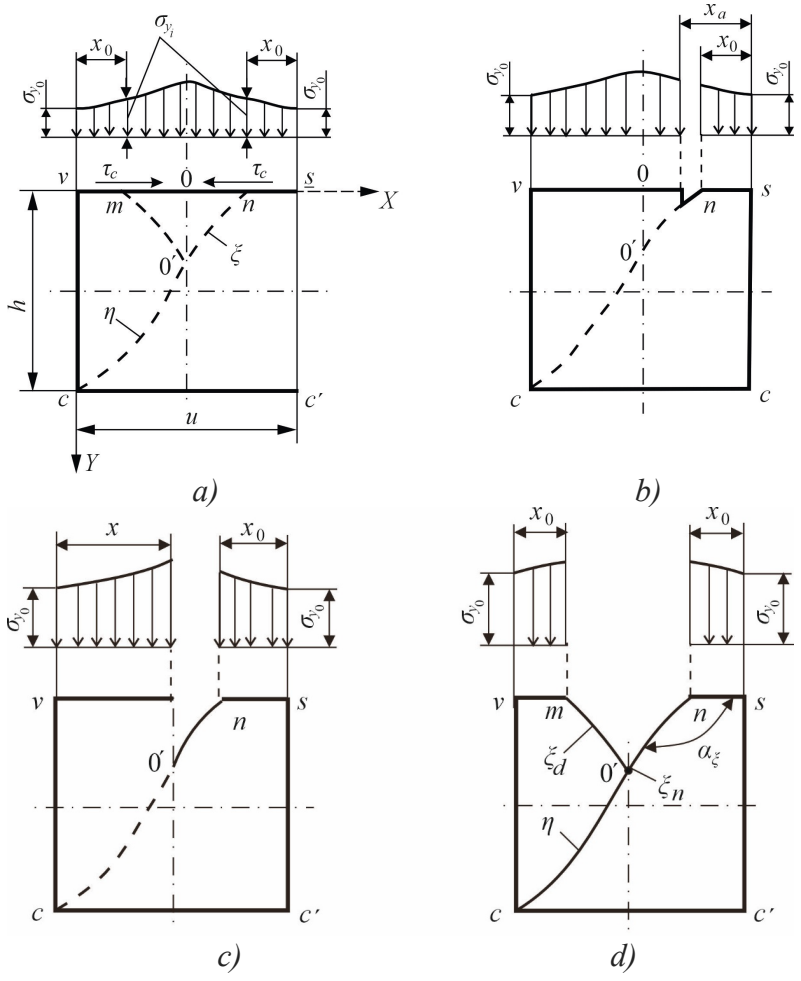

a) – at the moment of pre-fracture; b) – at the moment of wedge edge emergence; c) – at the moment of wedge edge formation; d) – at the moment of wedge formation

Figure 2 – Diagram of wedge formation during compression of a rock sample

The wedge shape appears on one of the halves of the contact plane and is charac-

terized by the intersection of the SS with the vertical plane of symmetry with a transition to the opposite side of the sample. First of all, it is necessary to determine the direction of crack development – from top to bottom or from bottom to top. Its formation is possible on the contact plane where the resistance to destruction is the lowest.

The essence of the problem remains unchanged if we consider the crack development in accordance with the diagram shown in Figure 2, starting from the upper horizontal plane on the right side of the sample. This approach is more intuitive. Based on the analysis of the figure, it can be noted that the interaction of a heterogeneous pair of sliding surfaces is considered: one of them is convex, and the other is concave. At the point of their contact, the stress values must be the same. This point of contact is point $O^{/}$ on the vertical plane of symmetry (Fig. 2), where the contact tangential stresses are zero. Let us imagine that a crack first forms at point *n*, at a distance x_o of from the right corner of the sample. According to our assumptions, based on the accepted scheme in Fig. 2, the crack develops along SS ξ_n, the second (left) of which connects at the moment when the crack reaches SS η, at the point where the load on it reaches a value exceeding that on *SS* ξ_d.

To describe the evolution of the wedge-shaped fracture of a cylindrical specimen, it is necessary to develop a law of contact stress distribution. For a prismatic specimen of unit width L. Prandtl, this law is represented by formula (1):

$$\sigma_{yi} = \sigma_{y_0}\left(1 + \frac{2f_k x}{h}\right), \tag{1}$$

where σ_{y_0} – is the vertical normal stress at the corner point of the sample, Pa; f_k – is the coefficient of contact friction; x – is the abscissa of the point under consideration, m; h – is the height of the sample, m.

Now we need to apply formula (1) to the area of the cylinder, but it must be different. Unlike the prismatic sample, in which the width of the sliding surface remains constant, in the cylindrical sample this surface expands all the time. Several models were tested in the study, but they did not give satisfactory results. Let us describe the proposed approach to the distribution law of contact normal stresses.

3. Results and discussion

First, let us write the formula for the circumference of a cylinder in the coordinate system $x - y$ (Fig. 3)

$$(x - r)^2 + y^2 = r^2, \tag{2}$$

where x and y – abscissa and ordinate of the point under consideration on the circle, m; r – radius of the cylinder circle, m.

Fig. 3 shows: O – the center of the sample circle; vY and vX – the axes of the coordinate system; φ – the angle of the segment solution, rad; a, b, c and d – points on the circle limiting the length of the chords.

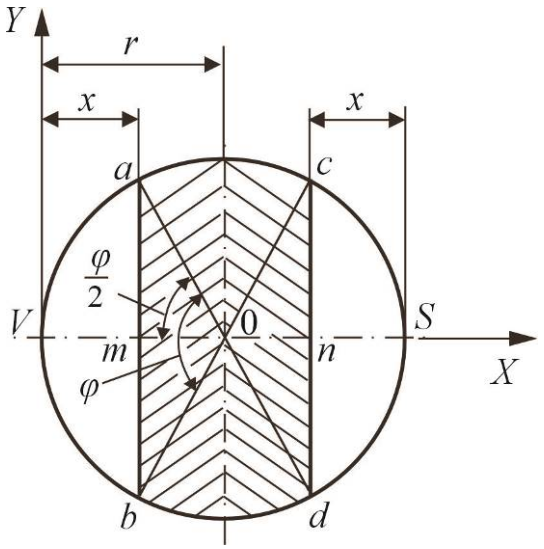

Figure 3 – Diagram showing the formation of the bearing area during the development of two symmetrical cracks in a cylindrical specimen

From the transformation of formula (2), we have

$$y = \sqrt{2rx - x^2}\,, \tag{2}$$

where y – ordinate of the chord points, m.

Then the formula for the length of the chord segment is

$$a = 2\sqrt{ux - x^2}\,, \tag{3}$$

where u – diameter of the circle, m.

Then, using expressions (1) and (3), we write down the formula for the distribution of vertical stress on the contact surface of a cylindrical sample, similar to L. Prandtl's formula for prismatic samples, while tying the abscissa x to one of the SS, for example, to the left SS ξ_l (Fig.2)

$$\sigma_{yi} = \sigma_y \left(\frac{2\sqrt{ux_\xi - x_\xi^2}}{u} + \frac{4f_k}{uh} x_\xi \sqrt{ux_\xi - x_\xi^2} \right). \tag{4}$$

Let us write down, according to expression (4), the formula for the force acting on the part of the sample that is not under load at the moment of crack development, as follows:

$$P = 2\sigma_y \int_0^x \left(\frac{\sqrt{ux_\xi - x_\xi^2}}{u} + \frac{2f_k}{uh} x_\xi \sqrt{ux_\xi - x_\xi^2} \right) dx, \qquad (5)$$

where σ_y – normal stress at the crack tip, Pa.

Now, using tabulated integrals, we will solve the integrals of formula (5), taking into account that, according to [13], the distribution functions of normal contact stresses for different SS (Fig. 2) have different forms:

at $x \geq 0.5u$

$$P = 2\sigma_y \left(\left((2-A)\frac{\sqrt{uA - A^2}}{4u} - \frac{1}{8u}\left(\frac{\pi}{2} - \arcsin 2\sqrt{uA - A^2} \right) \right) + \right.$$
$$\left. + \frac{2f_k}{uh} \left(-\frac{\left(uA - A^2\right)\sqrt{uA - A^2}}{3} + \frac{(2-1)\sqrt{uA - A^2}}{8} - \right.\right.$$
$$\left.\left. - \frac{1}{16}\left(\frac{\pi}{2} - \arcsin 2\sqrt{uA - A^2} \right) \right) \right), \qquad (6)$$

where $A = \left(x_0 + 0.5 - x_\xi\right)$.

at $x \leq 0.5u$

$$P = 2\sigma_y \left(\left((2B-1)\frac{\sqrt{uB - B^2}}{4u} - \frac{1}{8u}\left(\frac{\pi}{2} - \arcsin 2\sqrt{uB - B^2} \right) \right) + \right.$$
$$\left. + \frac{2f_k}{uh} \left(-\frac{\left(uB - B^2\right)\sqrt{u - B^2}}{3} + \frac{(2B-1)\sqrt{u - B^2}}{8} - \right.\right.$$
$$\left.\left. - \frac{1}{16}\left(\frac{\pi}{2} - \arcsin 2\sqrt{uB - B^2} \right) \right) \right), \qquad (7)$$

where $B = \left(0.5 - x_\eta\right)$.

To determine the specific force on the contact plane during crack propagation (beyond the elastic state), the force should be divided by the area not affected by the load. As a result, based on expressions (6) and (7), we determine the specific force on the load-bearing part of the sample, equal to $\pi u^2/4$, (the area of a circle), minus the area that is no longer under load during crack propagation,

at $x \geq 0.5u$

$$P=\sigma_y\left(\frac{\pi u^2}{4}-2\left(\left(\left(2A-1\right)\frac{\sqrt{uA-A^2}}{4u}-\frac{1}{8u}\left(\frac{\pi}{2}-\arcsin 2\sqrt{uA-A^2}\right)\right)+\right.\right.$$
$$\left.\left.+\frac{2f_k}{uh}\left(-\frac{\left(uA-A^2\right)\sqrt{uA-A^2}}{3}+\frac{\left(2-1\right)\sqrt{uA-A^2}}{8}-\right.\right.\right.$$
$$\left.\left.\left.-\frac{1}{16}\left(\frac{\pi}{2}-\arcsin 2\sqrt{uA-A^2}\right)\right)\right)\right)/, \quad (8)$$
$$\left(\frac{\pi u^2}{4}-\left(2A-1\right)\right)\frac{\sqrt{uA-A^2}}{4u}-\frac{1}{8u}\left(\frac{\pi}{2}-\arcsin 2\sqrt{uA-A^2}\right)$$

at $x \le 0.5u$

$$P=\sigma_y\left(\frac{\pi u^2}{4}-\left(\left(\left(2B-1\right)\frac{\sqrt{uB-B^2}}{4u}-\frac{1}{8u}\left(\frac{\pi}{2}-\arcsin 2\sqrt{uB-B^2}\right)\right)+\right.\right.$$
$$\left.\left.+\frac{2f_k}{uh}\left(-\frac{\left(uB-B^2\right)\sqrt{u-B^2}}{3}+\frac{\left(2B-1\right)\sqrt{u-B^2}}{8}-\right.\right.\right.$$
$$\left.\left.\left.-\frac{1}{16}\left(\frac{\pi}{2}-\arcsin 2\sqrt{uB-B^2}\right)\right)\right)\right)/, \quad (9)$$
$$\left(\frac{\pi u^2}{4}-\left(2B-1\right)\right)\frac{\sqrt{uB-B^2}}{4u}-\frac{1}{8u}\left(\frac{\pi}{2}-\arcsin 2\sqrt{uB-B^2}\right)$$

Next, we determine the stresses σ_y at the crack tip. We use the method described in article [13] for a prismatic specimen. The stress calculation system for the right SS ξ must be formulated taking into account the condition that there is no contact friction on the plane of symmetry

$$\begin{cases}\sigma_{y_\xi}=\dfrac{1}{\mu}\left(\dfrac{k_n\left(1+\sin\rho\sqrt{1-b_\xi^2}\right)\cdot\exp\left(2\mu\cdot\beta_\xi\right)}{1-\sin\rho}-k_0\right),\\ k_0=\dfrac{\left(\mu\sigma_{y_\xi}+k_n\right)\left(1-\sin\rho\sqrt{1-b_\xi^2}\right)}{\left(1+\sin\rho\right)}\end{cases} \quad (10)$$

where μ and $\rho=arctg\mu$ are the coefficient and angle of internal friction, rad; β_ξ is the angle of rotation of SS ξ from contact friction at the crack tip, rad; k_0 is the effective tangential stress at point O, Pa.

In this case, the following condition must be satisfied: $x_\xi \geq 0.5u$ and $x_\xi = u - x$.

The angle of inclination SS ξ is determined by the formula:

$$\alpha_\xi = \frac{3\pi}{4} - \frac{\rho}{2} + \beta_\xi . \tag{11}$$

Now let us consider the crack propagation along the left SS η at $x \leq 0.5u$. The stresses σ_{y_η} are determined by the system of equations

$$\begin{cases} \sigma_{y_\eta} = \dfrac{1}{\mu}\left(\dfrac{k_n\left(1+\sin\rho\sqrt{1-b_\eta^2}\right)\cdot\exp\left(-2\mu\left(\beta_\eta+\beta_c\right)\right)}{1-\sin\rho\sqrt{1-b_c^2}} - k_c \right), \\ k_c = \dfrac{\left(\mu\sigma_y + k_n\right)\left(1-\sin\rho\sqrt{1-b_\eta^2}\right)}{\left(1+\sin\rho\sqrt{1-b_c^2}\right)\cdot\exp\left(-4\mu\beta_c\right)} \end{cases} \tag{12}$$

where β_η and β_c – turn angles SS η from contact friction on the SS itself and on the lower contact plane at point c, rad;

In this case, the following condition must be observed: $x_\eta \leq 0.5u$, $x_\eta = x$.

The angle of inclination of the SS η is described by formula (13):

$$\alpha_\eta = \frac{3\pi}{4} - \frac{\rho}{2} + \beta_{\eta_л} . \tag{13}$$

Now, using the specific force acting on the load-bearing (non-deformed) part of the specimen, we proceed to calculate the stresses across its initial circular area, equal to $\pi u^2/4$.

Using formulas (8) and (9) together with expressions (10–13), the specific force values on the load-bearing part of the sample are calculated. Knowing these values, it becomes possible to determine the current values of deformations during crack growth, which is one of the key parameters of the “longitudinal stress-strain” diagram for uniaxial compression of specimens, according to the well-known formula:

$$\varepsilon = \frac{\rho}{E}, \tag{14}$$

where E – modulus of elasticity, Pa.

A straight line is constructed on the true diagram (Fig. 4) using formula (14).

Next, it is necessary to determine the value of the second parameter—the current strength of the sample on the critical branch of the conditional diagram. To do this, we multiply the specific force by the ratio of the bearing area of the sample to its initial area. The result of this multiplication should provide the initial stress value equivalent to the specific force and also reflect the decrease in strength on the limit branch of the diagram. To do this, we express the area under load as a segment (Fig. 3) using the known formula:

$$S_{ambd} = \frac{u^2}{8}(\varphi - \sin\varphi), \tag{15}$$

where φ – angle of the segment solution, rad.

Angle φ

$$\varphi = 2\arcsin\sqrt{1-\left(\frac{u-2x_\xi}{u}\right)^2}\,. \tag{16}$$

Then the area of the segment abv (Fig. 3) during crack propagation

$$S_{abv} = \frac{u^2}{8}(\varphi - \sin\varphi) = \frac{u^2}{4}\left(\arcsin 2\sqrt{ux_\xi - x_\xi^2} - 2(1-2x_\xi)\sqrt{ux_\xi - x_\xi^2}\right). \tag{17}$$

Then the bearing area of the sample circle

$$S_1 = \left(\frac{\pi u^2}{4} - \frac{u^2}{4}\left(\arcsin 2\sqrt{ux_\xi - x_\xi^2} - 2(1-2x_\xi)\sqrt{ux_\xi - x_\xi^2}\right)\right). \tag{18}$$

As a result of the research, the strength formula on the limit branch of the "longitudinal stress-strain" diagram is as follows:

$$\sigma_c = \frac{4\rho}{\pi u^2}\left(\frac{\pi u^2}{4} - \frac{u^2}{4}\left(\arcsin 2\sqrt{ux_\xi - x_\xi^2} - 2(1-2x_\xi)\sqrt{ux_\xi - x_\xi^2}\right)\right). \tag{19}$$

Using formulas (14) – (19) together with expressions (8–17), it is possible to determine, using the iteration method on a computer, the parameters of the true and conditional "longitudinal stress-strain" diagrams, which researchers obtain on presses with truncated wedge-shaped failure of cylindrical samples as a function of the limit branch $\sigma_c = \varphi(\varepsilon)$. Fig. 4 shows these functions for a modulus of elasticity E = 2000 MPa and various values of rock property indices for a sample with a height and diameter equal to one. An important conclusion can be drawn from the analysis

of the diagrams: the slope of the limit curve $\sigma_c = \Psi(\varepsilon)$, the so-called decay modulus M, which researchers take as a constant characteristic of the material similar to the elastic modulus E, depends on the numerical values of the rock property indices and is not a constant. To confirm this conclusion, branch 5 is shown in Fig. 4 at $f_k = 0$.

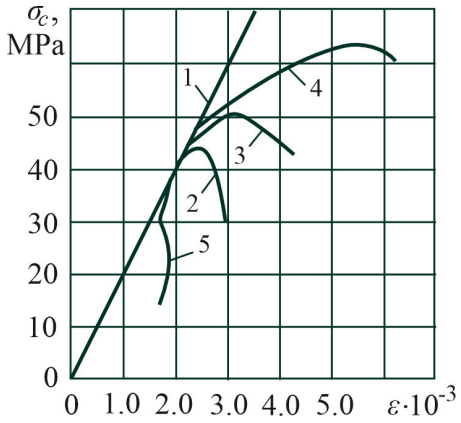

1 – true diagram; 2 – ρ=20°; 3 – ρ=30°; 4 – ρ=39°; 5 – ρ=20°, f = 0.

Figure 4 – Extreme wedge-shaped failure curves of samples at k_n = 10 MPa, f = 0.25, E = 2000 MPa

As can be seen in Fig. 4, there is a bend in the curves, and their linearity ends at low values of σ_c. Researchers indicate that with a wedge-shaped fracture and a load exceeding 50–70% of the maximum, there is significant nonlinearity. It should also be noted that in the initial part of the limit curve, there is a so-called hardening of the material according to the increasing curve, followed by its decline.

Many researchers explain the roundness of the limit branches of the diagrams by the plastic properties of rocks. However, in our opinion, this explanation does not correspond to reality. Rocks are highly brittle, and the roundness of the limit branches rather reflects the complex nonlinear relationships between stresses and areas released from the load during the formation of cracks. It is important to note that Hooke's law is observed on the load-bearing part of the sample (line 1), and the true diagram takes the form of a straight line, despite the presence of nonlinearities in the conditional diagrams.

To confirm the reliability of the proposed method, we will compare the calculated strength limit values with experimental data taken from the cadastre (Table 1). The average level of coincidence was 85.2%, which indicates a good degree of correspondence for rocks according to the method of assessing the convergence of calculated and experimental data developed by Prof. L.I. Baron.

4. Conclusions

Based on the results of the studies conducted, the following conclusions were formulated:

1. A mathematical model for calculating stress-strain diagrams for wedge-type rock failure has been developed, based on the use of four basic indicators of their physical properties: the shear strength of the material (k_n), the coefficients of contact

and internal friction (f and μ), and the modulus of elasticity (E). All these parameters can be experimentally determined in laboratory conditions using simple technical means available at production enterprises.

Table 1 – Comparison of calculated strength limits with experimental data for wedge-shaped failure of rock samples [17]

Rock type	Experimental			Calculated		Cadastre [6], p.
	τ_{sr}, MPa	ρ, degrees	σ_{comp}, MPa	σ_{comp}, MPa	Similarity, %	
argillite	4.0	35	24.0	22	84.6	172
sandstone	6.63	36	32.5	37	88.3	172
hornfels	25.0	39	138.0	158.0	89.1	66
shale	6.7	35	35.0	37.2	96.9	159
argillite	7.85	35	46.5	87.3	84.3	172
porphyry skarned diabase	15.0	37	78.5	87.3	91.7	66
argillite	5.0	30	24.0	30	88.3	171
siltstone	6.5	31	35.0	32.3	78.9	174
sandstone	10.0	30	55.0	48.2	74.2	158
limestone	12.0	30	60.0	58.2	82.2	158
marbled limestone	8.0	35	37.0	44.3	87.0	66
oxidized magnetite	20.0	32	97.0	103.2	93.8	66
heavily altered monazite	28.0	22	164	122	77.4	104
hematized tuff	25.0	36	134,0	145	97.8	67
garnet skarn	20.0	39	112.0	128	83,0	67
magnetite-garnet skarn	10.0	39	68.0	64.0	96.2	67
hornfel	16.0	34	84.0	85.0	96.5	67

2. Based on the maximum and minimum values of normal stresses recorded at the limit sections of the curve diagrams, the values of the limits and residual strength of the samples can be determined. These indicators are equivalent to analytical data calculated from diagrams of the dependence of normal stress on longitudinal deformation obtained on press equipment. Comparison of the calculated strength limits with the results of experiments confirmed the reliability of the developed method with an accuracy of 82–85%.

3. The proposed method will allow determining the parameters of stress-strain diagrams for cylindrical rock samples during their wedge-shaped failure. It is based on four material characteristics that can be easily determined during experiments directly at mining enterprises.

4. For the first time, the process of destruction of cylindrical rock samples caused by wedge-shaped destruction has been modeled, taking into account internal and external friction factors, the use of which will allow predicting and controlling the stress-strain state of the rock mass, ensuring the safe development of mining operations in the process of mining enterprises.

Conflict of interest

Authors state no conflict of interest.

REFERENCES

1. Nesmashny, E.A. and Bolotnikov, A.V. (2017), "Determining the strength of rock rocks using modern equipment on the example of the Bolshaya Glyvatka deposit", *Metallurhycheskaia I hornorudnaia promyshlennost*, vol. 3, pp. 82–87.

2. Bingxiang, H. and Jiangwei L. (2013), "The effect of loading rate on the behavior of samples composed of coal and rock", *Int J Rock Mech Min Sci.*, vol. 61, pp. 23–30. https://doi.org/10.1016/j.ijrmms.2013.02.002

3. Meyer, J.P. and Labuz, J.F. (2013), "Linear failure criteria with three principal stresses", *Int J Rock Mech Min Sci.*, vol. 60, pp. 180–187. https://doi.org/10.1016/j.ijrmms.2012.12.040

4 Tarasov, B. and Potvin, Yv. (2013), "Universal criteria for rock brittleness estimation under triaxial compression", *Int J Rock Mech Min Sci.*, vol. 59, pp. 57–69. https://doi.org/10.1016/j.ijrmms.2012.12.011

5. Chanyshev, A.I. (2010), "Boundary deformation of materials under anti-plane deformation and its consideration in the problem of propagation of a rectilinear semi-infinite crack", *Deformyrovanye y razrushenye materyalov s defektamy y dynamycheskye yavlenyia v hornykh porodakh y vyrabotkakh: materiali XX Mezhdunarodnoi nauchnoi shkoli* [Deformation and destruction of materials with defects and dynamic phenomena in rocks and workings: materials of the 20th International science schools], Simferopol, Ukraine, pp. 349–354.

6. Lavrikov, S.V. and Revuzhenko, A. F. (2016), "Deformation of geo-medium with considering for internal self-balancing stresses", *AIP Conference Proceedings*, vol. 1783, pp. 020130. https://doi.org/10.1063/1.4966423

7. Peng, Z. and Gomberg, J. (2010), "An integrated perspective of the continuum between earthquakes and slow-slip phenomena", *Nature Geoscience*, no. 3, pp. 599 – 607. https://doi.org/10.1038/ngeo940

8. Shashenko, A.N., Sdvijkova, E.A. and Gapeev, S.N. (2008), *Deformyruemost y prochnost massyvov hornykh porod* [Deformability and strength of rock masses], NSU of Ukraine, Dnipropetrovsk, Ukraine.

9. Shashenko, A.N., Sdvijkova, E.A. and Gapeev, S.N. (2008), *Deformatsyonnye modely v heomekhanyke* [Deformation models in geomechanics], NSU of Ukraine, Dnipropetrovsk, Ukraine.

10. Kovrov, A.S. (2009), "Modeling of the phenomenon of loss of stability of rock ledges on equivalent materials", *Naukovyi visnyk NHU*, vol. 9, pp. 48–56.

11. Brune, J.N. (1970), "Tectonic stress and the spectra of seismic shear waves from earthquakes", *J. of Geophysical Research*, vol. 75, issue 26, pp. 4997–5009. https://doi.org/10.1029/JB075i026p04997

12. Vasiliev, L.M., Vasiliev, D.L., Malych, N.G., and Angelovsky, A.A. (2018), *Mekhanyka obrazovanyia form razrushenyia obraztsov hornыkh porod pry ykh szhatyy. Monohrafiia* [Mechanics of Formation of Forms of Ruin of Rock Samples During Their Compression. Monograph], YMA-press, Dnipro, Ukraine.

13. Nesetova, V. and Lajtai, E.Z. (1973), "Fracture from compressive stress concentrations around elastic flaws", *Int. J. Rock Mech. Min. Sci. & Geomech. Abstr*, vol. 10, pp. 265–284. https://doi.org/10.1016/0148-9062(73)90038-7

14. Carter, B.J., Lajtai, E.Z. and Petukhov, A. (1991), "Primary and remote fracture around underground cavities", *Int. J. Numer. Anal. Meth. Geomech*., vol. 15, no. 1, pp. 21–40. https://doi.org/10.1002/nag.1610150103

15. Carter, B.J., Lajtai, E.Z. and Yuan, Y. (1992), "Tensile fracture from circular cavities loaded in compression", *Int. J. Fract*., vol. 57, no. 3, pp. 221–236. https://doi.org/10.1007/BF00035074

16. Yuan, Y.G., Lajtai, E.Z. and Ayari, M.L. (1993), "Fracture nucleation from a compression-parallel, finite-width elliptical flaw", *Int. J. Rock Mech. Min. Sci. & Geomech. Abstr.*, vol. 30, no. 7, pp. 873–876. https://doi.org/10.1016/0148-9062(93)90039-G

17. Vasiliev, L.M., Vasiliev, D.L. and Malych, N.G. (2016), "Analytical method for calculating the ultimate strength of prismatic rock samples with their wedge-shaped destruction", *Metallurhycheskaia I hornorudnaia promyshlennost*, vol. 6, pp. 65–70.

About the authors

Vasiliev Dmytro, Doctor of Technical Sciences (D.Sc.), Senior Researcher, Senior Researcher of Department of Mechanics of structures elastomeric mining machines, M.S. Poliakov Institute of Geotechnical Mechanics of the National Academy of Science of Ukraine (IGTM of the NAS of Ukraine), Dnipro, Ukraine, vasyliev.d.i.@dsau.dp.ua, ORCID ***0000-0001-6864-357X***

Tynyna Serhii, Candidate of Technical Sciences (Ph.D.), Senior Researcher, Senior Researcher of Department of Mechanics of structures elastomeric mining machines, M.S. Poliakov Institute of Geotechnical Mechanics of the National Academy of Science of Ukraine (IGTM of the NAS of Ukraine), Dnipro, Ukraine, serhgiu@gmail.com, ORCID ***0000-0002-9448-5488***

Kress Denys**,** Graduate Student, M.S. Poliakov Institute of Geotechnical Mechanics of the National Academy of Science of Ukraine (IGTM of the NAS of Ukraine), Dnipro, Ukraine, denni7777777@gmail.com ***(Corresponding author)***, ORCID ***0009-0001-9504-5695***

Rizo Zahar**,** Graduate Student, M.S. Poliakov Institute of Geotechnical Mechanics of the National Academy of Science of Ukraine (IGTM of the NAS of Ukraine), Dnipro, Ukraine, zaharrizo777@gmail.com, ORCID ***0000-0002-8271-7886***

Kulak Yevhen**,** Graduate Student, M.S. Poliakov Institute of Geotechnical Mechanics of the National Academy of Science of Ukraine (IGTM of the NAS of Ukraine), Dnipro, Ukraine, ievgenkulak@gmail.com, ORCID ***0009-0003-5931-9454***

АНАЛІТИЧНИЙ МЕТОД РОЗРАХУНКУ ПАРАМЕТРІВ ДІАГРАМ РОЗЧАВЛЮВАННЯ ЦИЛІНДРИЧНИХ ЗРАЗКІВ ГІРСЬКИХ ПОРІД ПРИ ЇХ КЛІНОПОДІБНІЙ ФОРМІ РУЙНУВАННЯ

Васильєв Д., Тинина С., Кресс Д., Різо З, Кулак Є.

Анотація. Управління напружено-деформованим станом масиву гірських порід дозволить спрогнозувати та забезпечити безпечний розвиток гірничих робіт у процесі експлуатації підприємств. Тому авторами встановлено, що однією з ключових характеристик, які є значущими для управління напружено-деформованим станом масиву гірських порід та забезпечення їх ефективного руйнування в процесі дезінтеграції, є показники межі міцності та залишкової міцності зразків. Дані параметри визначаються на основі діаграм, які відображають залежність нормальної напруги від поздовжньої деформації при граничному руйнуванні матеріалів. Також слід зазначити, що результати проведених досліджень необхідні безпосередньо на гірничому підприємстві для ухвалення рішення з урахуванням отриманої інформації про властивості гірських порід, а на самих об'єктах дане обладнання відсутнє. Мета статті – розробка аналітичного методу розрахунку параметрів діаграм розчавлювання циліндричних зразків гірських порід клинової форми їх руйнування для управління напружено-деформованим станом гірничого масиву та підвищення ефективності руйнування при дезінтеграції. Авторами в роботі аналітично проведено моделювання процесу руйнування циліндричних зразків гірських порід за їх клинової форми руйнування з використанням експериментальних значень чотирьох показників властивостей гірських порід – межі опору зсуву, коефіцієнтів внутрішнього і зовнішнього тертя, модуля пружності. Межі та залишкова міцність зразків еквівалентні аналітичним даним, які обчислюються за діаграмами залежності нормальної напруги від поздовжньої деформації, одержуваним на пресовому устаткуванні. Порівняння розрахункових меж міцності з наслідками експериментів підтвердило надійність розробленого методу з точністю не більше 82-85 %.

Вперше виконано аналітичне моделювання процесу руйнування циліндричних зразків гірських порід, що обумовлене клиноподібною формою руйнування, з урахуванням факторів внутрішнього та зовнішнього тертя. За результатами проведених досліджень встановлено, що запропонований метод дозволяє визначити параметри діаграм напруга-деформація циліндричних зразків гірських порід при їх клиновій формі руйнування з використанням чотирьох показників властивостей, які простими способами можуть бути експериментально в умовах гірничих підприємств, де результати розрахунку можуть бути оперативно використані для оцінки ефективності руйнування при дезінтеграції.

Ключові слова: гірська порода; межа міцності; руйнування; тріщина; діаграма "напруга-деформація".